

# Strong Magnetic Interactions and Short Range Magnetic Correlations in $\text{CuTeO}_4$

Zubia Hasan<sup>1</sup>, Michal J. Winiarski<sup>2</sup>, Kathryn E. Arpino<sup>3</sup>, Thomas Halloran<sup>1</sup>, Thao T. Tran<sup>4</sup>, and Tyrel M. McQueen<sup>1,5</sup>

<sup>1</sup>Institute for Quantum Matter, Department of Physics and Astronomy, The Johns Hopkins University, Baltimore, MD 21218

<sup>2</sup>Faculty of Applied Physics and Mathematics and Advanced Materials Center, Gdansk University of Technology, Narutowicza 11/12, 80- 233 Gdansk, Poland

<sup>3</sup> Max Planck Institute for Chemical Physics of Solids, 01187 Dresden, Germany

<sup>4</sup>Department of Chemistry, Clemson University, Clemson, SC 29634, USA

<sup>5</sup>Department of Chemistry and Department of Materials Science and Engineering, The Johns Hopkins University, Baltimore, MD, 21218

## Abstract

$\text{CuTeO}_4$  has been proposed as a crystallographically distinct, yet electronic structure analog, of superconducting cuprates. Magnetization measurements from  $T = 2\text{--}300$  K indicate the presence of antiferromagnetic, low dimensional correlations with  $J = 148(7)$  K. Below  $T \approx 50$  K, there is an upturn in magnetization indicative of enhanced ferromagnetic correlations, with neutron powder diffraction data showing the emergence of diffuse magnetic scattering at  $Q \approx 0.6 \text{ \AA}^{-1}$ . A Warren line shape analysis yields a characteristic magnetic correlation length of  $\xi = 4.5(9) \text{ \AA}$  at  $T = 40$  K, rising to  $\xi = 10.1(9) \text{ \AA}$  at  $T = 10$  K. Specific heat measurements reveal a sizable T-linear contribution of  $\gamma = 8.3 \text{ mJ/mol-f.u/K}^2$  at  $T < 5$  K. Together, these results imply a low dimensional, antiferromagnetic spin glass state. Structural modeling of the neutron powder diffraction data reveals the presence of a layered-type of stacking disorder, providing both a rationale for the lack of long range magnetic order, as well as being consistent with the computational predictions of its two-dimensional nature. Unlike the cuprates, we find no evidence of substantive dopability in this wide band-gap, yellow insulator.

## I Introduction

High temperature superconductivity in copper oxides is one of the most exciting emergent phenomena to result from strong electron correlations [1][2][3]. Significant progress has been made in the past 30 years in elucidating the key ingredients that underlie this behavior, with a layered, two-dimensional electronic structure, strong Cu-d and O-p orbital hybridization, and proximity to an insulating, magnetically ordered state, all believed to be important.

Recent computational work [4] identified  $\text{CuTeO}_4$  as a previously unrecognized material containing these ingredients. Figure 1 shows the reported crystal structure of  $\text{CuTeO}_4$ , highlighting the layered nature that is distinct from the cuprates

in not being built of free-standing  $\text{CuO}_2$  planes but rather highly angled, corner sharing  $\text{CuO}_4$  units, arranged as coupled 1D chains, with the Cu-O-Cu bond angle of  $126.1^\circ$  closer to herbertsmithite [5] than to the cuprates. Thus  $\text{CuTeO}_4$  gives a possible new avenue to expand the known cuprate families, and provides an opportunity to test which features are most important in ultimately producing superconductivity.

Despite being known for more than 40 years [6], there is scant experimental data on  $\text{CuTeO}_4$ , particularly with regards to its magnetic and electronic properties. This is likely due to the difficulty in preparation, which required hydrothermal conditions at  $650^\circ\text{C}$  and 2000 bar for two months, to produce a multiphase mixture containing small crystals of  $\text{CuTeO}_4$ .

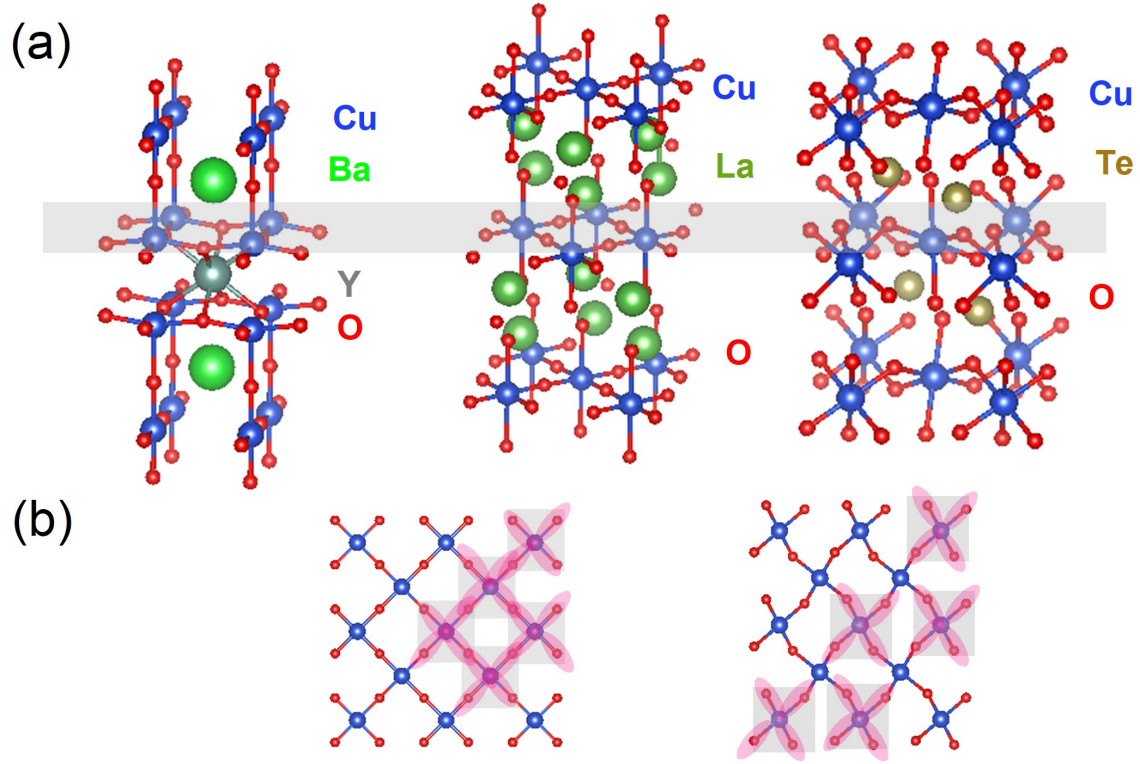


Figure 1: (a) Comparison of the layered structures of known superconductors  $\text{La}_2\text{CuO}_4$  [7] and  $\text{YBa}_3\text{Cu}_2\text{O}_7$  [8] to  $\text{CuTeO}_4$ . (b) While all structures have 2D  $\text{CuO}_2$  planes with  $\text{CuO}_4$  units (grey squares)  $\text{CuTeO}_4$  has strong buckling driven by shared oxygens with  $\text{TeO}_6$  octahedra. The alternating  $\text{CuO}_4$  plaquettes in  $\text{CuTeO}_4$  suggest a 1D chain like behaviour, mediated through  $d_{x^2-y^2}$  orbitals lying in the same plane.

By developing a simpler, less onerous, route to preparing  $\text{CuTeO}_4$ , utilizing mild hydrothermal conditions at  $210^\circ\text{C}$  for 7 days, we are able to overcome these limitations. Here, we report on the low temperature magnetic behavior of  $\text{CuTeO}_4$ , utilizing a combination of magnetization, specific heat, and neutron powder diffraction measurements. The magnetization measurements show a broad hump at  $T = 148(7)$  K, suggesting some low dimensional antiferromagnetic correlations. Elastic neutron scattering reveals diffuse scattering at  $Q \approx 0.6 \text{ \AA}^{-1}$ , which alongside bifurcations at  $T \approx 50$  K in zero field cooled (ZFC) and field cooled (FC) susceptibility measurements imply that  $\text{CuTeO}_4$  is a low dimensional, antiferromagnetic spin glass compound. Low temperature specific heat measurements for  $T < 5$  K shows a large T-linear contribution of  $\gamma = 8.3 \text{ mJ/mol f.u./K}^2$ , which is

unexpected for a wide band gap insulator but is consistent with a spin glass state.

## II Methods

$\text{CuTeO}_4$  was initially synthesized by Falck et al [6] under high pressure and temperature. We report a novel method of synthesizing yellow, polycrystalline  $\text{CuTeO}_4$  in mild hydrothermal conditions. A 1 : 3 ratio of  $\text{CuO}$  (2 mmol) and  $\text{Te}(\text{OH})_6$  (6 mmol) was used to make the reaction mixture. This was placed in a 23 ml Teflon lined stainless steel autoclave with 10 ml water and 0.03 ml  $\text{H}_2\text{O}_2$ .<sup>1</sup> A magnetic stir bar was added to the Teflon Cup and the autoclave was closed and placed on a magnetic hot plate in a sandbath. A temperature of  $210^\circ\text{C}$  was maintained for 7 days with the help of a thermocouple placed next to the autoclave in the sand. A difference of a

<sup>1</sup>The inclusion of  $\text{H}_2\text{O}_2$  seems to be crucial for the formation of  $\text{CuTeO}_4$  in such mild conditions. Repetition of this experiment without  $\text{H}_2\text{O}_2$  resulted in the formation of  $\text{Cu}_3\text{TeO}_6$ , the more thermodynamically favourable phase in the formation of  $\text{CuTeO}_4$ . The decomposition of  $\text{CuTeO}_4$  into  $\text{Cu}_3\text{TeO}_6$  alongside  $\text{TeO}_2$  and  $\text{O}_2$  at  $510^\circ\text{C}$  is documented in [9].  $\text{H}_2\text{O}_2$  quenches this decomposition by preventing the formation of  $\text{TeO}_2$ , oxidizing  $\text{Te}^{4+}$  to  $\text{Te}^{6+}$ .

few degrees from the thermocouple sensing and the temperature within the autoclave was expected.

The phase purity of  $\text{CuTeO}_4$  was confirmed by Powder X-ray diffraction data (PXRD) collected at room temperature. This was done using Bruker D8 Focus diffractometer with a LynxEye detector and  $\text{Cu K}\alpha$  radiation ( $1.54 \text{ \AA}$ ). Rietveld refinements on the PXRD data were done through TOPAS 4.2 [10][11].

The Magnetic Susceptibility was collected using the Vibrating Sample Magnetometer option in the Quantum Design Physical Properties Measurement System (PPMS) at a temperature range of 2 - 300 K. The susceptibility is defined by the relation  $\chi \approx \frac{M}{H}$  where  $M$  is the Magnetization of the sample and  $H$  is the applied field. The specific heat of the sample was measured using the semiadiabatic pulse method in the PPMS equipped with a Dilution Refrigerator from  $T = 0.1 - 300 \text{ K}$ . Powder Neutron Diffraction data was obtained using the high-resolution neutron powder diffractometer POWGEN, Frame 2, center wavelength  $1.5 \text{ \AA}$  and  $6 \times 10^7$  total counts at the Oak Ridge National Laboratory. Stacking faults in the material were simulated using DIFFaX v 1.813 [12].

### III Results

#### A Magnetism

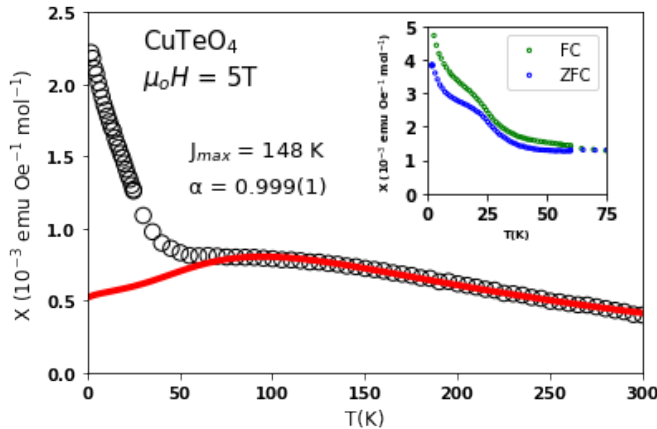


Figure 2: Molar magnetic susceptibility of  $\text{CuTeO}_4$  fit to a  $S=\frac{1}{2}$  Alternating Exchange Heisenberg Chain (red line). Inset shows ZFC/FC splitting indicative of a spin glass state.

The temperature dependent magnetic susceptibility data of  $\text{CuTeO}_4$  shows no 3D long range ordering as

displayed in Fig. 2. Furthermore, there is no region in the susceptibility data that could be fit with the Curie-Weiss model. However, it seems there may be a paramagnetic regime at  $T \geq 150 \text{ K}$ ,

Parameters	Fit
$K \text{ (erg Oe}^{-2} \text{ mol}^{-1})$	$7.30(8) \times 10^{-3}$
$J_{max} \text{ (K)}$	$148(7)$
$\alpha$	$0.999(1)$
$\chi_o \text{ (emu Oe}^{-1} \text{ mol}^{-1})$	$-2.62(2) \times 10^{-4}$

Table 1: Fit parameters for  $T > 65 \text{ K}$  for the magnetic susceptibility data (Figure2).

as seen in some low-dimensional magnets [13][14][15]. The magnetic behaviour of  $\text{CuTeO}_4$  is similar to  $\text{Na}_2\text{Cu}_2\text{TeO}_6$  which displays paramagnetic behaviour at  $T > 300 \text{ K}$  [16]. We find that for  $T > 65 \text{ K}$ , the data for  $\text{CuTeO}_4$  is well fit by a two dimensional function for the  $S=\frac{1}{2}$  Antiferromagnetic Alternating Exchange Heisenberg chain [17], using the expression,

$$\chi(T) = K\chi^*(\alpha, \frac{T}{J_{max}}) + \chi_o \quad (1)$$

where  $K = \frac{N_A g^2 \mu_B^2}{J_{max} k_B}$  is an overall scaling factor,  $\chi_o$  is the temperature-independent term and  $\chi^*$  is the AFM alternating exchange model as a function of reduced temperature  $\frac{T}{J_{max}}$ .  $\chi^*(\alpha, \frac{T}{J_{max}})$  describes a Heisenberg chain with two antiferromagnetic exchange interactions  $J_1$  and  $J_2$ , with  $J_2 \leq J_1$  and  $\alpha = \frac{J_2}{J_1}$ . When  $\alpha=0$ , the model recovers the isolated spin dimer model and when  $\alpha=1$ , the model recovers the uniform AFM Heisenberg chain. The values from the best fit are given in Table 1.  $\alpha = 0.999(1)$  indicates highly uniform exchange interactions and suggests that at  $T > 65 \text{ K}$ ,  $\text{CuTeO}_4$  behaves as system of 1D AFM spin chains. This is perhaps surprising in the context of the prior discussion of twisted  $\text{CuO}_2$  planes, but in agreement with a detailed view of the crystal structure, Figure 1(b), which shows how the particular connectivity of  $\text{CuO}_4$  plaquettes forms 1D chains within each plane. The value of  $g = 1.7(3)$  appears slightly lower than the expected value of 2.2, but the large uncertainty precludes more definitive interpretation.  $J_{max} = 148(7) \text{ K}$ , is consistent with the experimental data, where a broad maximum is observed around the same temperature range. This value of  $J$  is roughly half of that expected from the Cu-O-Cu bond

angle [18]; this likely reflects the greater ionicity of the Cu-O bonds in  $\text{CuTeO}_4$  due to the large inductive withdrawing effect of neighboring  $\text{Te}^{6+}$  ions [19]. The negative value of  $\chi_o$  is consistent with the insulating behavior of the compound. The abrupt upturn at  $T = 50$  K is suggestive of a magnetic transition, with some ferromagnetic correlations. To confirm the freezing behaviour of this compound at  $T = 50$  K, field-cooled (FC) and zero field-cooled (ZFC) DC susceptibility data was taken at  $\mu_o H = 1$  T for  $\text{CuTeO}_4$  (Figure 2). The bifurcation between ZFC and FC data at  $T \approx 50$  K shows that there is some freezing taking place at that transition temperature.

To unequivocally determine the glassy behaviour of  $\text{CuTeO}_4$ , time of flight, elastic neutron scattering was carried out for  $\text{CuTeO}_4$  at  $T = 10$  K, 40 K, 60 K and 120 K. No Bragg peaks were observed in the data, but instead at  $Q \approx 0.6(\text{\AA}^{-1})$ , there is a broad peak (Figure 3) that emerges, suggestive of short range magnetic order. Further evidence that it is magnetic in nature comes from subtracting the high temperature data from the low temperature data, Figure 4. The excess scattering falls off with angle, which implies a magnetic, rather than nuclear, form factor. The peak center is  $Q \approx 0.6 \text{\AA}^{-1}$ . This position is same as the one expected for (010) reflection,  $0.61 \text{\AA}^{-1}$ . As this reflection is disallowed for the nuclear structure due to systematic absences, it is likely this scattering is magnetic in nature and indicates the formation of short range magnetic order, with AFM order along the b axis (perpendicular to the planes). An alternative interpretation that we cannot definitively rule out is that this reflects the appearance of magnetic order with a propagation vector of  $k = (0.5, 0, 0)$  ( $Q = 0.57 \text{\AA}^{-1}$  for the first peak), but that seems unlikely as the standard crystallographic cell of  $\text{CuTeO}_4$  can accommodate in-plane magnetic order without enlarging the unit cell. The breadth of this peak is well-described by a Warren lineshape [20], which is characteristic of short range order along that crystallographic direction. The Warren lineshape function is,

$$P_{2\theta} = C \frac{1 + \cos^2 2\theta}{2(\sin \theta)^{\frac{3}{2}}} \frac{\sqrt{\pi}}{2e^{a^2}} \quad (2)$$

where  $C = KmF_{hk}^2 \frac{L}{\lambda\sqrt{\pi}}$ ,  $d = \frac{2L\sqrt{\pi}}{\lambda}$  and

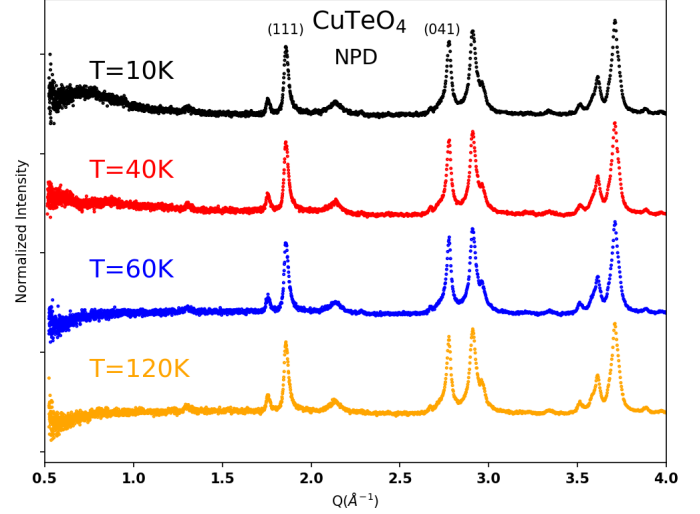


Figure 3: Raw elastic neutron scattering data for  $T=10$  K, 40 K, 60 K and 120 K. No magnetic bragg peaks are visible. The structure peaks like (111) and (041) remain the same at different temperatures. At low  $Q$  ( $\text{\AA}^{-1}$ ) we can see a broad peaks emerging at low temperature indicative of short range magnetic order.

$a = d(\sin(\theta) - \sin(\theta_o))$ . Here  $K$  is the overall scale factor,  $F_{hk}$  is the structure factor,  $m$  is the multiplicity of reflection (hk) centered around  $2\theta_o$  and  $L$  is the average correlation length. The extracted correlation length is  $\xi = 4.5(9) \text{\AA}$  at 40 K, rising to  $\xi = 10.1(9) \text{\AA}$  at 10 K, Table 2. The value of  $\theta_o$  for  $T = 10$  K is in agreement with the experimental data in Figure 3, where the broad peak appears at  $Q \approx 0.6(\text{\AA}^{-1})$ . The fit for  $T = 40$  K was constrained to this  $\theta_o$  value for the function in Figure 4. The correlation lengths at  $T = 10$  K and 40 K, are close to the interlayer spacing within  $\text{CuTeO}_4$ , and suggests little coherence between distinct planes of chains. Thus we conclude that  $\text{CuTeO}_4$  exhibits glassy behavior with short correlation lengths between planes.

T (K)	C	$\theta_o$ (°)	L (Å)
10	0.732(5)	5.07(1)	10.1(9)
40	0.505(3)	5.07(1)	4.5(9)

Table 2: Fit parameters with the statistical portion of error from the Warren lineshape .

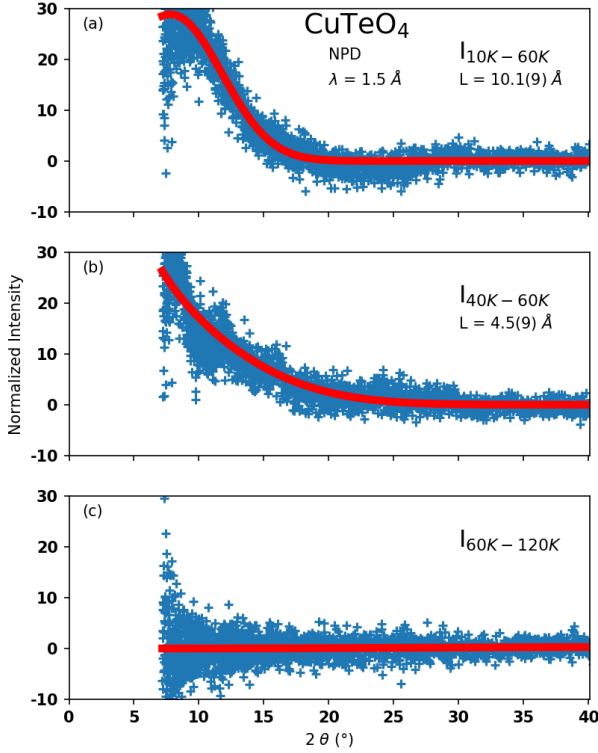


Figure 4: Warren Lineshape analysis characterizing short range order in  $\text{CuTeO}_4$ . The fit is shown by the solid red line while the subtracted experimental data (a) 10 K - 60 K (b) 40 K - 60 K are the scattered blue markers, (c) 60 K - 120 K is included to show the absence of short range correlations in the spin glass state after the freezing temperature of  $T \approx 50$  K.

## B Heat Capacity

To further elucidate the physical properties of  $\text{CuTeO}_4$ , temperature-dependent specific heat measurements were carried out. Figure 5 shows the specific heat characterization of  $\text{CuTeO}_4$  from 0.1 - 300 K. No sharp transitions are seen in this temperature range indicating a lack of long range magnetic order as shown by elastic neutron scattering and magnetic susceptibility data discussed previously. The experimental data is well fit at  $T \geq 4$  K by two Debye modes modelled by the following equation:

$$\frac{C_p}{T} = \frac{D(\theta_{D1}, T)}{T} + \frac{D(\theta_{D2}, T)}{T} \quad (3)$$

The fit was constrained so that  $C_{\text{phonon}}(T) \leq C(T)$  at higher temperatures so that the phonon contribution is not overestimated. The oscillator strength as well as the two Debye temperatures are shown in Table 3. The first debye mode peaks approximately at  $T \approx 50$  K, which is around  $T_g$ , this is similar to other spin glasses where the maximums are observed after or at  $T_g$  [21][22][23]. While no sharp maximums are observed in the specific heat data, this may be simply due to a more gradual entropy loss which does not result in any sharp transitions. While, within this temperature range the expected Dulong-Petit value of  $3nR$  is not recovered, this can be explained by the high value of  $\theta_{D2}$  which means that  $C(T)$  will plateau at  $T \geq \theta_{D2}$ . The low temperature specific heat,  $T \leq 4$  K is modelled by  $\frac{C_p}{T} = \beta T^2 + \gamma$  where we extract  $\gamma = 8.30(4) \text{ mJ mol}^{-1} \text{ K}^{-2}$  and  $\beta = 0.46(2) \text{ mJ mol}^{-1} \text{ K}^{-4}$ . This value of  $\beta$  recovers  $\theta_D = 293.3$  K, closer to  $\theta_{D1}$  than  $\theta_{D2}$ .

Parameter	Fit
$\theta_{D1}$ (K)	257(1)
$s_{D1}$	1.78(2)
$\theta_{D2}$ (K)	794(13)
$s_{D2}$	4.08(6)

Table 3: Experimental data is well fitted with two debye modes. The oscillator strength ( $s_{D1}$ ,  $s_{D2}$ ) add up to 5.86, just shy of 6 atoms per formula unit found in  $\text{CuTeO}_4$ .

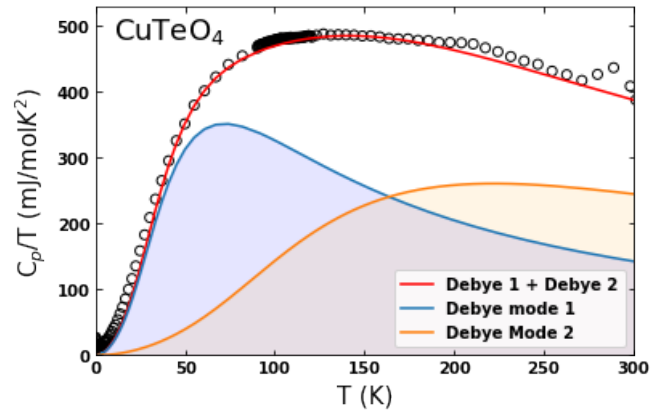


Figure 5: Specific heat measurements modelled by two Debye modes, with  $\theta_{D1}$  dominant at low temperatures. The small transition at 275 K is due to the vaporization of n-grease.



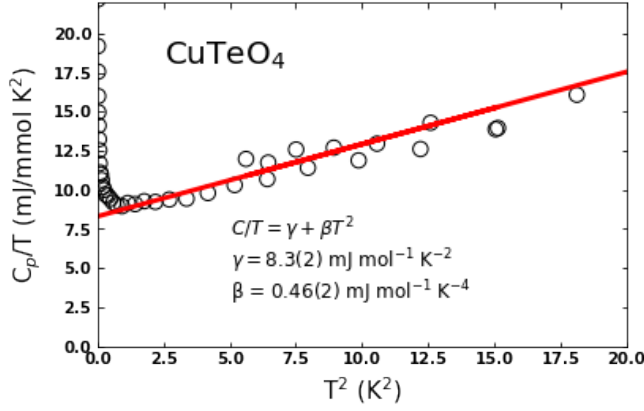


Figure 6: low temperature specific heat measurements of  $\text{CuTeO}_4$ .

This agrees with our Debye heat capacity analysis as at low temperatures the first Debye mode has a larger contribution to the specific heat as shown in Figure 5. The T-linear contribution to heat capacity is shown in Figure 6. At low temperatures, the phonon contribution to the specific heat often scales as the dimensionality of the material. The  $T^3$  contribution to the heat capacity therefore suggests that the phonon dispersions of  $\text{CuTeO}_4$  are fairly three dimensional. The  $\gamma$  term, despite the material being a large band gap insulator, can be attributed to the large number of available magnetic states at low temperature rather than electronic states [24][25][26]. This is consistent with other reported spin glass compounds, where at  $T \leq T_g$ , the heat capacity scales as  $T$  [21][22]. While we have qualitatively described the magnetic contribution to heat capacity, it should be noted that  $C_{\text{magnetic}}$  cannot be quantitatively extracted from the specific heat data as the phonon contribution cannot be distinguished from the magnetic contribution due to lack of a non magnetic analog for  $\text{CuTeO}_4$ .

### C Crystal Structure

With the magnetic properties of  $\text{CuTeO}_4$  firmly established, an obvious question arises: why is there short-range, glassy order, with an extremely short correlation length between  $\text{CuO}_2$  planes? To answer this, we investigated the crystal structure in greater detail using powder x-ray diffraction. Falck et al. previously characterized the crystal structure in the  $P2_1/n$  spacegroup [6]. Rietveld refinement of this model to our powder diffraction data (Figure 7a), shows clear discrepancies, especially in the predicted

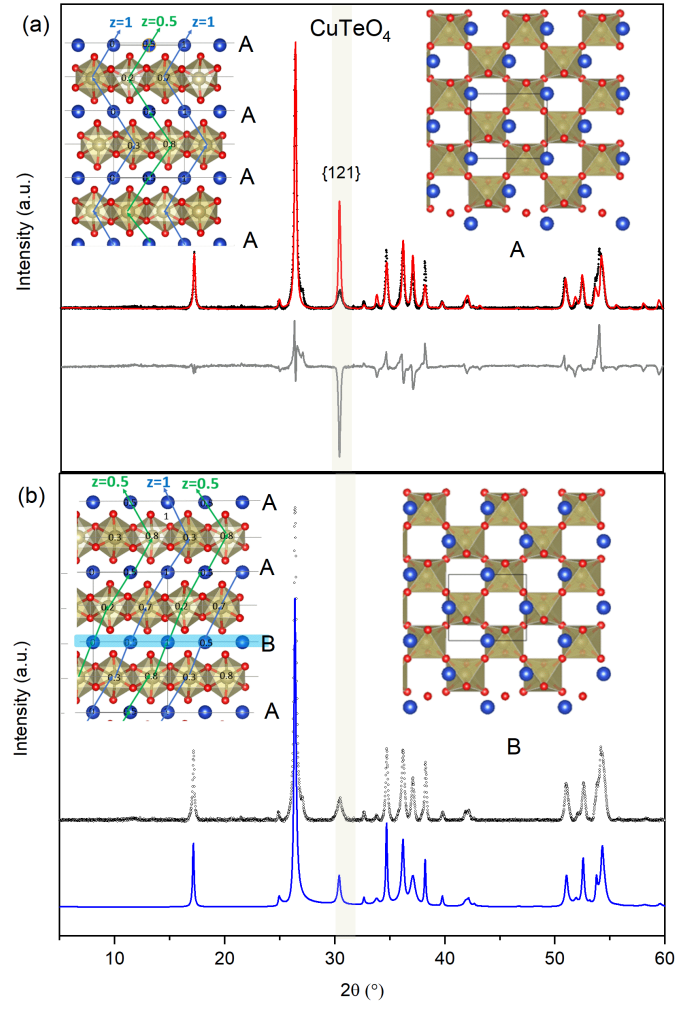


Figure 7: (a) Rietveld refinement (red line) of powder x-ray diffraction data (black). The (121) peak is poorly fitted by the  $P2_1/n$  model. Inset in (a) shows a layered view of  $\text{CuTeO}_4$  in  $P2_1/n$  (left) and a planar view (right) of the 'A' stacking model. (b) The model with 70% original Cu stacking and 30% altered-Cu position layering (blue line) is a good qualitative fit to x-ray data (black), capturing the breadth and height of the (121) peak. Inset in (b) shows the faulted stacking, highlighted in blue (left) and a planar view of the faulted layer 'B' (right).

intensity of the (121) peak, indicating this model is an incomplete description of the structure. The (121) peak is an allowed reflection specifically due to the Cu atoms on  $P2_1/n$  Wyckoff positions 2a and 2c, which prompted an investigation into Cu disorder. The potential of possible stacking disorder is further supported by (1) the inconsistent broadening of peaks in our experimental diffraction data, (2) the higher symmetry which is suggested

by  $\gamma = 90^\circ$  in the monoclinic  $P2_1/n$  model but which could not be solved in a spacegroup, and (3) Falck et al.’s report [6] that their  $P2_1/n$  model could also be described as the  $\text{TeO}_4$  layers belonging to spacegroup  $Pnma$  along with the lower-symmetry Cu atoms possessing only n-glide symmetry. We posit based on the structure model that a plane of Cu atoms might occur on  $P2_1/n$  Wyckoff positions 2b and 2d instead of 2a and 2c (Inset Fig. 7a,7b). While the two are similar, Cu atoms in the faulted plane have a slightly greater overlap with the Te-O coordination octahedra of the underlying layer. As both original and faulted Cu planes have the same intralayer arrangement, the subsequent  $\text{TeO}_4$  layer positions identically with respect to the Cu. Using DIFFaX, we simulated models with 0-100% alternate Cu planes and found a probability of 70% original and 30% faulted Cu planes (Fig. 7b) is in good agreement with the experimental data. We note that because the fault is extended over an entire plane, post-synthetic measures such as annealing would be dynamically insufficient to resolve the structure to the  $P2_1/n$  “ideal.”

## IV Conclusion

$\text{CuTeO}_4$  was proposed as a high  $T_c$  candidate amongst other copper tellurates due to its crystal structure and antiferromagnetic, insulating ground state which is similar to other superconducting cuprates. While  $\text{CuTeO}_4$  was predicted to have a 2D antiferromagnetic ground state [4], our experiments have shown  $\text{CuTeO}_4$  to display 1D AFM chain behavior at  $T > 65$  K, due to the  $\text{CuO}_4$  plaquettes highlighted in Figure 1. First principles calculations in [4] showed  $\text{CuTeO}_4$  to have a small bandgap of 0.13 eV, increasing to 1 eV upon inclusion of a Hubbard U, making it a suitable candidate for superconductivity upon doping. However, the yellow colour of the polycrystalline powder qualitatively suggests a much larger band gap than the one proposed. While the GGA functional used for the calculations is known to underestimate the band gap, upon closer inspection of the band structures it seems that the origin of the underestimation is not solely due to the exchange correlation functional used. We propose that the large difference in experimental and predicted band gap may be due to the failure of DFT to consider the effect of hypervalent cations like

$\text{Te}^{6+}$  which have a strong inductive withdrawal effect on  $\text{O}^{2-}$ . This also explains the apparent undopability of the parent structure as attempts to dope  $\text{CuTeO}_4$  with Sb were unsuccessful due to the covalent character of the TeO bond. Thus, we have shown  $\text{CuTeO}_4$  to be an undopable, yellow, wide band-gap insulator.  $\text{CuTeO}_4$  harbors a spin glass state with  $T_g$  occurring at  $T = 50$  K as shown by (i) bifurcation in ZFC and FC magnetic susceptibility measurements at  $T = 50$  K (ii) Low temperature specific heat measurements which reveal a sizable T-linear contribution of  $\gamma = 8.3(1)$  mJ/mol f.u./K<sup>2</sup>, consistent with other reported spin glasses. (iii) Elastic neutron scattering showing diffuse peaks at  $Q \approx 0.6 \text{ \AA}^{-1}$  at  $T = 10$  K and  $T = 40$  K, which flatten out at  $T = 60$  K and  $T = 120$  K, indicating a freezing transition in between the two temperature ranges. Warren line shape analysis reveals short range correlations, with average magnetic correlation length of  $\xi = 10.1(9) \text{ \AA}$  at  $T = 10$  K, decreasing to  $\xi = 4.5(9) \text{ \AA}$  at  $T = 40$  K. The spin glass behavior of  $\text{CuTeO}_4$  can be explained by its disordered layering as shown by the x-ray powder diffraction data. Simulating the disordered layering reveals a qualitative fit to disorder in copper positions which disturbs the stacking pattern.

While it is unclear, if the stacking faults are the thermodynamically stable state for this compound, lack of layering faults would not change its undopable, wide band gap insulating nature which is mainly due to the hypervalency of  $\text{Te}^{6+}$  ions. Therefore, our characterization of  $\text{CuTeO}_4$  as an undopable, wide band gap insulator, rules out high temperature superconductivity in copper tellurates where Te is found in the  $\text{Te}^{6+}$  state. Furthermore, it presents new opportunities to explore high temperature superconductivity in copper tellurates where there is a reduced inductive withdrawal effect by Te, such as those compounds where Te is present in the 4+ state, thus making them better suited candidates for doping.

## V Acknowledgements

This work was supported as part of the Institute for Quantum Matter, an Energy Frontier Research Center funded by the U.S. Department of Energy, Office of Science, Office of Basic Energy Sciences, under Award DE-SC0019331.

K.E.A acknowledges support from the Humboldt Foundation Postdoctoral Fellowship. T.T.T acknowledges support from Clemson University, College of Science, Department of Chemistry.

## References

- [1] Elbio Dagotto. Correlated electrons in high-temperature superconductors. *Rev. Mod. Phys.*, 66:763–840, Jul 1994.
- [2] N. P. Armitage, P. Fournier, and R. L. Greene. Progress and perspectives on electron-doped cuprates. *Rev. Mod. Phys.*, 82:2421–2487, Sep 2010.
- [3] A critical review of selected experiments in high- $T_c$  superconductivity. *Physica B: Condensed Matter*, 169(1):7 – 16, Feb 1991.
- [4] Antia S. Botana and Michael R. Norman. Electronic structure of  $\text{CuTeO}_4$  and its relationship to cuprates. *Phys. Rev. B*, 95:115123, Mar 2017.
- [5] Matthew P. Shores, Emily A. Nytko, Bart M. Bartlett, and Daniel G. Nocera. A structurally perfect  $s = 1/2$  kagomé antiferromagnet. *Journal of the American Chemical Society*, 127(39):13462–13463, 2005.
- [6] L. Falck, O. Lindqvist, W. Mark, E. Philippot, and J. Moret. The crystal structure of  $\text{CuTeO}_4$ . *Acta Crystallographica Section B*, 34(5):1450–1453, May 1978.
- [7] G. H. Lander, P. J. Brown, C. Stassis, P. Gopalan, J. Spalek, and G. Honig. Magnetic and structural study of  $\text{La}_{1.8}\text{Sr}_{0.2}\text{NiO}_4$ . *Phys. Rev. B*, 43:448–456, Jan 1991.
- [8] A. A. R. Fernandes, J. Santamaria, S. L. Bud'ko, O. Nakamura, J. Guimpel, and Ivan K. Schuller. Effect of physical and chemical pressure on the superconductivity of high-temperature oxide superconductors. *Phys. Rev. B*, 44:7601–7606, Oct 1991.
- [9] G. G. Gospodinov. Phase states of copper orthotellurates in an aqueous medium and in thermolysis. *J. Mater. Sci. Lett*, 11:1460–1462, Jan 1992.
- [10] J. Perl, J. Shin, J. Schumann, B. Faddegon, and H. Paganetti. TOPAS: An innovative proton Monte Carlo platform for research and clinical applications. *Medical Physics*, 39:6818, 2012.
- [11] B. Faddegon, J. Ramos-Mendez, J. Schuemann, A. McNamara, J. Shin, J. Perl, and Paganetti H. The TOPAS Tool for Particle Simulation, a Monte Carlo Simulation Tool for Physics, Biology and Clinical Research. *Physica Medica*, 2020.
- [12] J.M.Newsam M.M.J Treacy, M.W.Deem. *DIFFaX manual*.
- [13] Daisuke Urushihara, Sota Kawaguchi, Koichiro Fukuda, and Toru Asaka. Crystal structure and magnetism in the  $S = 1/2$  spin dimer compound  $\text{NaCu}_2\text{VP}_2\text{O}_{10}$ . *IUCrJ*, 7(4):656–662, Jul 2020.
- [14] N. Motoyama, H. Eisaki, and S. Uchida. Magnetic susceptibility of ideal spin  $1/2$  heisenberg antiferromagnetic chain systems,  $\text{Sr}_2\text{CuO}_3$  and  $\text{SrCuO}_2$ . *Phys. Rev. Lett.*, 76:3212–3215, Apr 1996.
- [15] P Khuntia and A V Mahajan. Magnetic susceptibility and heat capacity of a novel antiferromagnet:  $\text{LiNi}_2\text{P}_3\text{O}_{10}$  and the effect of doping. *Journal of Physics: Condensed Matter*, 22(29):296002, jun 2010.
- [16] Jianxiao Xu, Abdeljalil Assoud, Navid Soheilnia, Shahab Derakhshan, Heather L. Cuthbert, John E. Greedan, Mike H. Whangbo, and Holger Kleinke. Synthesis, structure, and magnetic properties of the layered copper(ii) oxide  $\text{Na}_2\text{Cu}_2\text{TeO}_6$ . *Inorganic Chemistry*, 44(14):5042–5046, 2005.
- [17] D. C. Johnston, R. K. Kremer, M. Troyer, X. Wang, A. Klümper, S. L. Bud'ko, A. F. Panchula, and P. C. Canfield. Thermodynamics of spin  $s = 1/2$  antiferromagnetic uniform and alternating-exchange heisenberg chains. *Phys. Rev. B*, 61:9558–9606, Apr 2000.
- [18] X. Rocquefelte, K. Schwarz, and P. Blaha. Theoretical investigation of the magnetic exchange interactions in copper(ii) oxides under chemical and physical pressures. *Sci Rep*, 2, Oct 2012.



- [19] J. Etourneau, J. Portier, and F. M  nil. The role of the inductive effect in solid state chemistry: how the chemist can use it to modify both the structural and the physical properties of the materials. *Journal of Alloys and Compounds*, 188:1 – 7, 1992.
- [20] B. E. Warren. X-ray diffraction in random layer lattices. *Phys. Rev.*, 59:693–698, May 1941.
- [21] K. Binder and A. P. Young. Spin glasses: Experimental facts, theoretical concepts, and open questions. *Rev. Mod. Phys.*, 58:801–976, Oct 1986.
- [22] K. H. Fischer. Spin glasses (i). *physica status solidi (b)*, 116(2):357–414, 1983.
- [23] A. P. Ramirez, G. P. Espinosa, and A. S. Cooper. Elementary excitations in a diluted antiferromagnetic kagom   lattice. *Phys. Rev. B*, 45:2505–2508, Feb 1992.
- [24] Loi T. Nguyen, T. Halloran, Weiwei Xie, Tai Kong, C. L. Broholm, and R. J. Cava. Geometrically frustrated trimer-based mott insulator. *Phys. Rev. Materials*, 2:054414, May 2018.
- [25] Itamar Kimchi, Adam Nahum, and T. Senthil. Valence bonds in random quantum magnets: Theory and application to  $\text{ybmga}_4$ . *Phys. Rev. X*, 8:031028, Jul 2018.
- [26] Li. Zhao, Tian-Wey Lan, Kuen-Jen Wang, Chia-Hua Chien, Tsu-Lien Hung, Jiu-Yong Luo, Wei-Hsiang Chao, Chung-Chieh Chang, Yang-Yuan Chen, Maw-Kuen Wu, and Christine Martin. Multiferroicity in geometrically frustrated  $\alpha\text{-mcr}_2\text{o}_4$  systems ( $m = \text{ca, sr, ba}$ ). *Phys. Rev. B*, 86:064408, Aug 2012.